Journal of Organometallic Chemistry 693 (2008) 2153–2158

Contents lists available at ScienceDirect

Journal of Organometallic Chemistry

journal homepage: www.elsevier.com/locate/jorganchem

A ruthenium(II) allenylidene complex with a 4,5-diazafluorene functional group: A new building-block for organometallic molecular assemblies

Olivier Pélerin, Céline Olivier, Thierry Roisnel, Daniel Touchard *, Stéphane Rigaut *

UMR 6226 CNRS, Université de Rennes 1, Sciences Chimiques de Rennes, Campus de Beaulieu, F-35042 Rennes Cedex, France

ARTICLE INFO

Article history:
Received 21 February 2008
Received in revised form 11 March 2008
Accepted 11 March 2008
Available online 16 March 2008

Keywords:
Ruthenium
Allenylidene
Diazafluorene
α-Diimine complexes
Carbon-rich bridges

ABSTRACT

The synthesis of the new ruthenium(II) allenylidene complex $[ClRu(dppe)_2{=}C{=}C{=}C_{11}H_6N_2][OTf]$ (**4**) (dppe = 1,2-bis(diphenylphosphino)ethane) terminated with a 4,5-diazafluorene ligand is reported. Further coordination of that metal allenylidene to ruthenium and rhenium moieties leads to the bimetallic adducts $[ClRu(dppe)_2{=}C{=}C{=}C_{11}H_6N_2\{Ru(bpy)_2\}][B(C_6F_5)_4]_3$ (**5a**), $[ClRu(dppe)_2{=}C{=}C{=}C_{11}H_6N_2\{Ru(^tBu\text{-}bpy)_2\}][PF_6]_3$ (**5b**) and $[ClRu(dppe)_2{=}C{=}C{=}C_{11}H_6N_2\{Re(CO)_3Cl\}][OTf]$ (**6**). Their optical and electrochemical properties show that the allenylidene moiety is an attractive molecular clip for the access to larger original redox-active homo/heteronuclear multi-component supramolecular assemblies. The X-ray crystal structure of the allenylidene metal building block is also described.

1. Introduction

Over the past decade, coordination complexes in which rigid linear π-conjugated organic chains span transition metal centres have been proposed as models for molecular wires or for molecular scale electronic devices and memories [1–4]. In particular, electron transfer processes between two redox centres have been examined with a wide range of systems [5–17], and transition metal complexes of the type [M]–C≡C–R–C≡C–[M] with direct connection of a carbon-rich bridge with metal centres have shown excellent abilities to complete a strong electronic interaction between the two remote redox-active metal centres [11–17]. Interestingly, less attention has been focused on related cumulenic species such as metal allenylidenes $[M]{=}C{=}C{=}CR_2$ [18–22] despite their potential in material science for molecular wires [23–30], probably for synthetic reasons.

Using the fragment $[ClRu(dppe)_2]^+$ (dppe = 1,2-bis(diphenylphosphino)ethane), our group has been involved in the building of new mono and polymetallic cumulenic species with unusual topologies and reversible redox behaviour that are potential molecular wires [17,18,30]. In particular, this system offers (i) an easy synthesis of bimetallic complexes containing two conjugated communicating ruthenium allenylidene centres [28], and (ii) access to a monometallic *trans*-$[Ph_2C{=}C{=}C{=}Ru(dppe)_2{=}C{=}C{=}CR_2]^{2+}$ system promoting efficient electronic delocalization between the two carbon-rich allenylidene chains in a *trans* arrangement [27]. More specifically, these complexes can be easily reduced, and mono-electronic reduction has been shown to lead to paramagnetic species with the single electron delocalized over the carbon-rich chain(s).

In this context, it is very appealing to build multi-metallic assemblies made from this cumulenic *trans* ditopic structure $[ClRu(dppe)_2{=}C{=}C{=}CR_2]^+$ that allow substitutions of the chlorine atom with a cumulenic or an acetylide [31] chain to obtain innovative conductive [32] or magnetic [33] organometallic networks. In order to bring these individual units together within a larger assembly designed for a specific task, it is essential to be able to control the spatial arrangement of both the ligands and the metal centres relative to each other. The incorporation of functionalized allenylidene ligands with a coordinating group such as a α-diimine moiety may represent an additional building tool that would open avenues for the construction of new homo and heteronuclear organometallic compounds important for functional materials [34,35]. Indeed, α-diimine metal complexes represent an attractive class of chromophores as they offer a large range of metals with different oxidation states and ligands that can give rise to tuneable optical, magnetic, and electrochemical properties. For example, end-capping of unsaturated organic spacers with redox-active groups, such as Ru(II) polypyridine metal centres, have been most studied where they are intended to promote long-range electron or energy transfer [2,8–10,36,37], and efficient octupolar architecture for NLO properties [38]. Rhenium(I) tricarbonyl diimine complexes have also been particularly widely used as building blocks because of their well-known photophysical, photochemical, and redox

* Corresponding authors. Tel.: +33 2 23 23 57 67.
E-mail addresses: daniel.touchard@univ-rennes1.fr (D. Touchard), stephane.rigaut@univ-rennes1.fr (S. Rigaut).

0022-328X/$ - see front matter © 2008 Elsevier B.V. All rights reserved.
doi:10.1016/j.jorganchem.2008.03.014

properties [10,39], including in carbon-rich multimetallic assemblies [40,41] and switches [42].

Herein, we describe the preparation, characterization, as well as the optical and electrochemical properties of a ruthenium allenylidene complex bearing a 4,5-diazafluorene functional group, along with those of other new species resulting from the coordination of the terminal diimine moiety to ruthenium and rhenium metal units as a proof of principle. The diazafluorene ligand [43–46] was preferred to the bipyridyl moiety [24] for its planar configuration, in order to provide increased stability to the reduced form of the allenylidene metals. The X-ray crystal structure of the allenylidene metal building block has been determined.

2. Results and discussion

2.1. Synthesis

The synthetic procedure to the new allenylidene metals is depicted on Scheme 1. This route follows the guideline previously established in the laboratory for this type of complex with the $Ru(dppe)_2$ system [31]. The actual propargylic alcohol **2** used to obtain the allenylidene complex bears a 4,5-diazafluorene group, and was readily obtained from 4,5-diazafluoren-9-one (**1**) and acetylene [47]. Further reaction of **2** with the 16 electron precursor $[RuCl(dppe)_2]OTf$ (**3**) led to the deep red allenylidene complex **4** bearing the 4,5-diazafluorene terminal group (83%), fully characterized by means of IR, NMR, mass spectroscopies, and elemental analysis [48]. The *trans* structure of the ruthenium centre is first established in the ^{31}P NMR spectrum which shows a singlet at 37.2 ppm for the 4 equiv. phosphorus atoms. The allenylidene nature of the chain is demonstrated with characteristic ^{13}C NMR signals at $\delta = 320.8$ (C_α), 247.0 (C_β), and 147.2 (C_γ) ppm. A typical intense vibration stretch ($\nu_{C=C=C}$) is also observed on the IR spectrum at 1915 cm^{-1}.

Good quality crystals were obtained from a methylene chloride/diethyl-ether/*n*-pentane triphasic mixture (2/1/4). Therefore, the X-ray structure of **4** could be resolved, and an ORTEP drawing of the cation with relevant atom labelling is depicted in Fig. 1. Experimental crystallographic data are given in Table 1, and selected bond lengths and angles in Table 2. The global structure of **4** consists in one cation unit, a triflate anion, and one CH_2Cl_2 as inclusion solvent [49]. Examination of the chain reveals that the Ru1–C10, C11–C12, C12–C13 distances are in line with typical values found in metal allenylidenes such as $[(\eta^5\text{-}C_5H_5)(PMe_3)_2Ru{=}C{=}C{=}CPh_2]PF_6$ [50]. The structure also evidences the almost linear arrangement of the bridge and of the chlorine atom both connected to the metal with a typical Cl1–Ru1–C10 angle of 176.57(9)° [29], although the carbon rich-chain is slightly more bent than usual at the C12 atom (C10–C11–C12 = 172.4(4)°). On the other hand, the diazafluorene moiety is planar as expected, and displays typical bond lengths and angles [51]. It is worth noting that the latter is not hindered at all by the dppe ligand; therefore it should tolerate further coordination.

The complexation of **4** was performed with Ru and Re metal fragments. In a first attempt, **4** was reacted with $Ru(bpy)_2Cl_2$ (bpy = 2,2′-bipyridine) in refluxing ethanol. The bimetallic adduct **5a** was obtained as a brown powder (79%). As expected the ^{31}P NMR resonance at 36.2 ppm was slightly shifted to higher field by comparison with that of **4**. The $\nu_{C=C=C}$ was observed at 1899 cm^{-1}. This band is less intense than that of the precursor. This phenomenon is tentatively attributed to the two positively charged centres that are expected to decrease the dipole moment change during the symmetric stretch [52]. Unfortunately, the compound appeared to be poorly soluble despite the use of $(C_6F_5)_4B^-$ as coun-

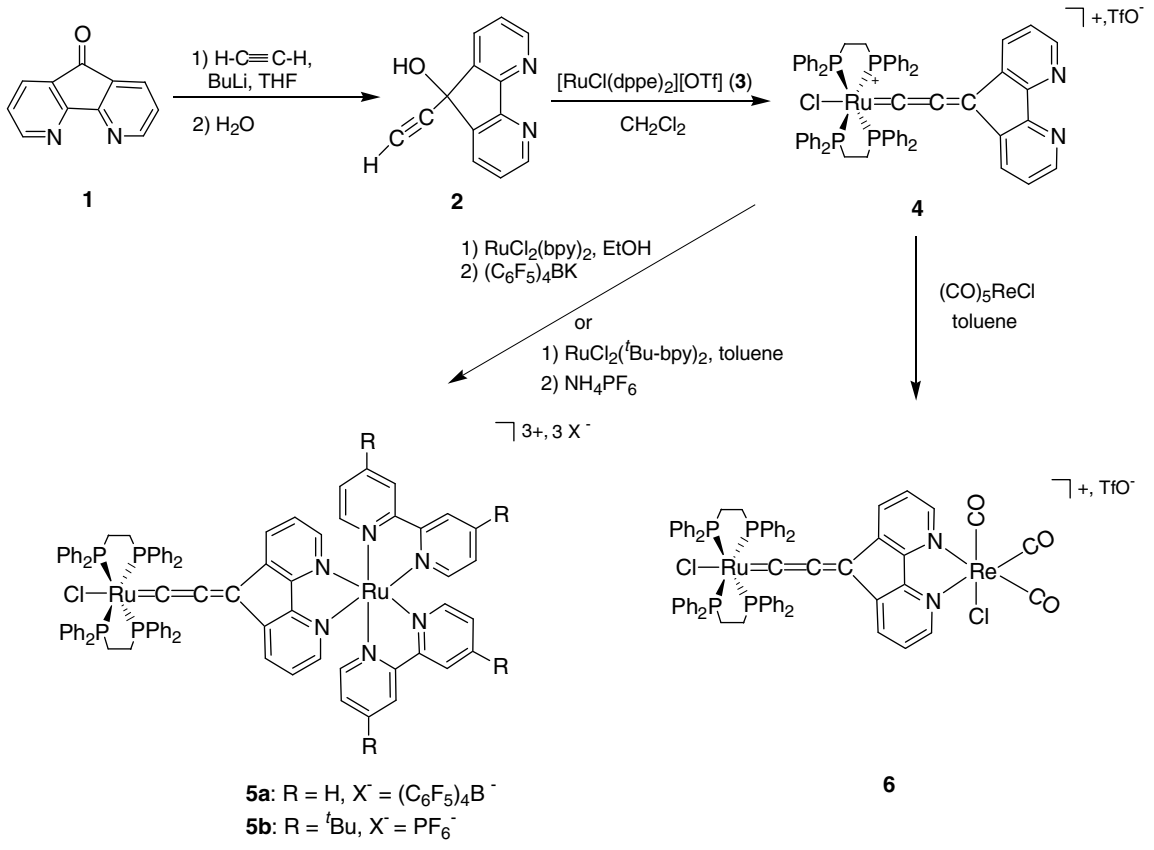

Scheme 1. Synthetic pathway for the allenylidene complexes.

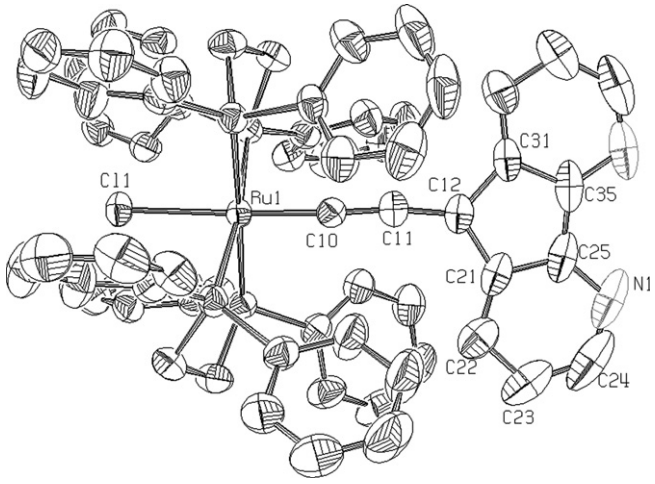

Fig. 1. Perspective view of the cation of **4**; thermal ellipsoids are set at 50% probability.

Table 1
Crystal data and structure refinement for **4**

Empirical formula	$C_{67}H_{56}Cl_3F_3N_2O_3P_4RuS$
Formula weight	1357.50
Temperature (K)	293(2)
Wavelength (Å)	0.71073
Crystal system, space group	Monoclinic, $P\,21/c$
Unit cell dimensions	
a (Å)	18.6734(2)
b (Å)	17.9871(2)
c (Å)	19.3233(3)
α (°)	90
β (°)	99.3950(10)
γ (°)	90
Volume (Å^3)	6403.26(14)
Z, Calculated density (Mg/m^3)	4, 1.408
Absorption coefficient (mm^{-1})	0.559
$F(000)$	2776
Crystal size (mm)	$0.58 \times 0.52 \times 0.44$
θ Range for data collection (°)	3.03–27.48
Limiting indices	$-24 \leqslant h \leqslant 24$, $-21 \leqslant k \leqslant 23$, $-25 \leqslant l \leqslant 25$
Reflections collected/unique [R_{int}]	27145/14633 [0.0211]
Completeness to $\theta = 27.48$ (%)	99.7
Absorption correction	None
Refinement method	Full-matrix least-squares on F^2
Data/restraints/parameters	14633/0/775
Goodness-of-fit on F^2	1.066
Final R indices [$I > 2\sigma(I)$]	$R_1 = 0.0494$, $wR_2 = 0.1413$
R indices (all data)	$R_1 = 0.0656$, $wR_2 = 0.1538$
Largest difference in peak and hole (e Å^{-3})	1.115 and −0.732

ter anion. As this might preclude future formation of larger assemblies, the ligation was also carried out with the Ru(^{t}Bu-bpy)Cl$_2$ (^{t}Bu-bpy = 4,4′-^{t}Bu$_2$-2,2′-bpy). The analogous soluble bi-metallic adduct **5b** was obtained in 77% yield. This complex displays similar spectroscopic characteristics, i.e. the ^{31}P NMR resonance at 36.1 ppm and the 1900 cm^{-1} $\nu_{=C=C=C}$. Furthermore, the ^{1}H NMR spectrum displays two expected signals at $\delta = 1.53$ ppm and 1.49 ppm for the ^{t}Bu groups.

Coordination of **4** was also completed with Re(CO)$_5$Cl using classic conditions [53]. After reaction for 18 h in refluxing toluene, the hetero-bimetallic complex **6** was obtained in good yield (67%). The ^{31}P NMR spectrum shows a singlet at 35.5 ppm for the 4 equiv. phosphorus atoms. The vibration stretch for the allenylidene chain ($\nu_{C=C=C}$) is observed in the IR spectrum at 1897 cm^{-1}, in addition to the expected ν_{CO}. The structures of all complexes are also supported by high resolution mass spectroscopy and ^{13}C NMR (when soluble).

Table 2
Selected bond lengths d (Å) and angles ω (°) in **4**

Bond	d	Bond	d
Ru(1)–Cl(1)	2.4441(7)	C(21)–C(25)	1.405(5)
Ru(1)–C(10)	1.873(3)	C(22)–C(23)	1.394(6)
C(10)–C(11)	1.261(4)	C(23)–C(24)	1.388(9)
C(11)–C(12)	1.342(4)	C(24)–N(1)	1.329(8)
C(12)–C(21)	1.473(5)	C(25)–N(1)	1.331(5)
C(12)–C(31)	1.480(5)	C(25)–C(35)	1.464(6)
C(21)–C(22)	1.354(6)		
Angle	ω	Angle	ω
C(10)–Ru(1)–Cl(1)	176.56(9)	C(25)–C(21)–C(12)	108.2(3)
C(11)–C(10)–Ru(1)	175.7(3)	C(21)–C(22)–C(23)	116.9(5)
C(10)–C(11)–C(12)	172.5(3)	C(22)–C(23)–C(24)	118.7(5)
C(11)–C(12)–C(21)	126.6(3)	N(1)–C(24)–C(23)	125.7(4)
C(11)–C(12)–C(31)	126.9(3)	N(1)–C(25)–C(21)	124.6(5)
C(21)–C(12)–C(31)	106.4(3)	N(1)–C(25)–C(35)	126.5(4)
C(22)–C(21)–C(25)	119.9(4)	C(21)–C(25)–C(35)	109.0(3)
C(22)–C(21)–C(12)	131.9(3)		

2.2. UV–Vis spectra

Typical UV–Vis absorption spectra are displayed in Fig. 2, and the band positions as well as the corresponding absorption coefficients are reported in Table 3. All spectra are dominated in the UV region by ligand-centred $\pi \rightarrow \pi^*$ transitions. These Intra Ligand transitions (IL) involve at least the dppe ligand, the allenylidene carbon-rich ligand, and its diazafluorene moiety [51,52]. For complex **4**, two broad absorption bands are also observed at lower energy. On the basis of the transitions observed for [ClRu(dppe)$_2$=C=C=CPh$_2$][PF$_6$] (**A**) (Table 3) [26], the absorption located at $\lambda_{max} = 521$ nm is expected to arise from the allowed transition from one of the metal based HOMOs to the allenylidene ligand based LUMO ($Ru^{II}(d\pi) \rightarrow \pi^*$(allenylidene), MLCT) [52]. The red shift is attributed to the electron withdrawing character of the diazafluorene moiety that lowers the allenylidene ligand orbital energy. The higher energy absorption at $\lambda_{max} = 453$ nm is tentatively assigned to a transition involving the diazafluorene group [51].

The bimetallic adducts **5a** and **5b** display very similar absorption spectra as expected. As an example, **5b** shows a high energy behaviour consistent with bipyridine IL transitions expected around 240 and 284 nm in addition to other ligand-centred $\pi \rightarrow \pi^*$ features. The set at lower energy obviously includes multiple bands as well. The detailed interpretation of such an absorption spectrum is difficult due to the overlapping of the bands. Indeed, mixed diimine ligands lower the symmetry of the complex and remove the degeneracy of the π^* levels which result in the appearance a broad MLCT band. Furthermore, the allenylidene contribution is expected in the same region. Nevertheless, the peak observed here at $\lambda_{max} = 469$ nm is similar in shape to those observed for $Ru^{II}(d\pi) \rightarrow \pi^*$(diimine) transition (MLCT) in ruthenium complexes coordinated to two bipyridines and to analogous 4,5-diazafluorene ligands (e.g. 4,5-diazafluoren-9-one) [44,45]. The present absorption band is red shifted by comparison with the latter, a phenomenon tentatively ascribed to the electron withdrawing character of the carbon-rich moiety. The low energy shoulder is larger and more intense than that observed in those analogous examples, a fact attributed to the presence of the $Ru^{II}(d\pi) \rightarrow \pi^*$(allenylidene) MLCT from metal allenylidene moiety in addition to the spin forbidden triplet absorption of the diazafluorene/bpy ruthenium centre. It is

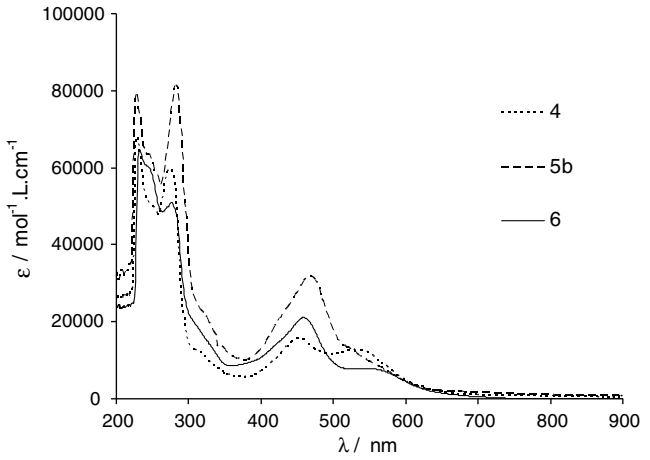

Fig. 2. UV–Vis absorption spectra for compounds **4**, **5b**, and **6** in CH_2Cl_2 solutions.

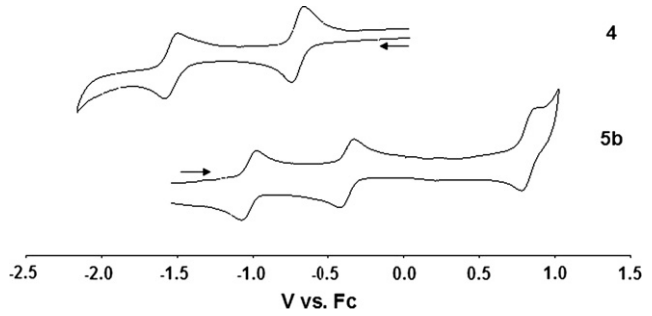

Fig. 3. Cyclic voltammograms of compounds **4** and **5b** recorded in CH_2Cl_2 solution containing $[NBu_4]PF_6$ at scan rate of 0.1 V/s.

Table 3
Electrochemical (CV) and UV–Vis data

	Electrochemistry[a]				UV–Vis[e]
	E°_{red3}	E°_{red2}	E°_{red1}	E°_{ox1}	λ_{max}/nm (ε/mol^{-1} L cm^{-1})
A		−2.11[c]	−1.03[b]	0.99[d]	230 (58300), 273 (59100), 505 (20100)
4		−1.38[d]	−0.58[b]		228 (68300) 274 (59900), 453 (15700), 521 (13700)
5a	−1.94[c]	−0.91[d]	−0.27[b]	1.03[b]	230 (96800) 284 (73200), 470 (25400)
5b	−2.11[c]	−0.94[d]	−0.29[b]	0.89[d]	230 (76000) 284 (86300), 469 (31800)
6		−1.05[d]	−0.32[b]	1.07[c]	232 (62500) 276 (49400), 458 (21110), 545 (sh, 8000)

[a] Sample 1 mM in CH_2Cl_2, $[NBu_4]PF_6$ (0.1 M), v = 100 mV s^{-1}, potentials are reported in V vs. ferrocene as an internal standard.
[b] Reversible oxidation processes, $\Delta E_p \approx 60$ mV.
[c] Peak potential of a chemically irreversible process.
[d] $\Delta E_p \approx 70$ mV.
[e] In CH_2Cl_2.

worth to note that the lowest energy MLCT transitions of ruthenium diimine complexes are known to be related to the difference between the first one-electron oxidation (Ru^{III}/Ru^{II}) and the first one-electron reduction (bpy/bpy$^{\cdot-}$) potentials ($\Delta E_{1/2}$) of this centre [54]. Electrochemical data (vide infra) were used to calculate the expected energy transitions for the relevant MLCT bands. As a result, the concerned MLCT transition is expected to result from the Ru(dπ) → bpy(π*) transition rather than from the Ru(dπ) → diazafluorene (π*) that should occur in the near-IR region of the spectrum. However, no absorptions were observed in this region showing that this transition should be forbidden as already reported [45].

The rhenium complex **6** displays a similar behaviour to that of **4** at high energy. At lower energy, the broad band centred at 458 nm is tentatively assigned as the Re(dπ) → π*(diazafluorene) MLCT transition, red shifted from the usual absorption owing to the presence of the positively charged allenylidene ligand [46]. However, the extinction coefficient on the order of 10^4 mol^{-1} L cm^{-1} is larger by an order of magnitude from the 10^3 mol^{-1} L cm^{-1} commonly observed for rhenium diimine MLCT transitions. Therefore this absorption band should probably also include a transition involving the cumulenic diazafluorene moiety as observed for complex **4**, transition which should also be buried in the broad low energy band in **5a,b** spectra. Finally, the low energy shoulder at λ_{max} = 545 nm is ascribed to the slightly red sifted Ru^{II}(dπ) → π*(allenylidene) MLCT. Overall, the optical properties of the different building blocks are retained in the bimetallic species.

2.3. Electrochemical data

Cyclic voltammetry (CV) was used to study the electrochemical behaviour of all metal complexes (CH_2Cl_2 solutions, 0.1 M Bu_4NPF_6). The values of the potentials for all compounds are reported in Table 3, and typical CVs are displayed in Fig. 3. Regarding the monometallic metal allenylidene **4**, the two reversible monoelectronic waves are attributed to the reduction of the cumulenic ligand [26,28,55]. As expected, the associated potentials at E° = −0.58 and E° = −1.38 V vs. Fc are more favourable than those of **A** because of the presence of *N*-atoms more electronegative than C-atoms in the diimine part. Importantly this planar diazafluorene group obviously enhances stability of the second reduced species. In contrast with **A**, and as a consequence of the positive shift of the potentials, no Ru^{II}/Ru^{III} oxidation event is observed in the electrochemical window [52].

Coordination of the chelating ligand with transition metals also considerably favour these reduction processes. Indeed, for the three bimetallic complexes **5a**,**b**–**6**, the first reduction occurs around $E^\circ \approx -0.30$ V, and the second around $E^\circ \approx -1.00$ V vs Fc. For the ruthenium complexes **5a**,**b**, the third irreversible reduction process is assigned to the reduction of the bipyridine ligands (not shown). On the other hand, the oxidation process observed for **5a**,**b** is reversible and attributed to the Ru^{II}/Ru^{III} oxidation of the ruthenium diimine moieties. Due to the electron withdrawing character of the allenylidene metal, this potential is slightly shifted by comparison to that of $Ru(bpy)^{2+}_3$ [10]. It is worth noting that these assignations are further supported by the significant negative shift of the third reduction and of the first oxidation observed for **5b** bearing two ^{t}Bu-bpy ligands by comparison with those of **5a**. Regarding the rhenium complex **6**, the irreversible oxidation process at E° = 1.07 V is tentatively associated with a metal-centred electrochemical reaction Re(I) → Re(II) [56]. Overall, these studies highlight the increased stabilization of the easily reduced metal allenylidenes by comparison with **A**, either with the free or coordinated diazafluorene ligand.

3. Conclusion

In this work, we have obtained a new allenylidene ruthenium complex bearing a chelating 4,5-diazafluorene ligand. Further coordination of this new molecular clip to ruthenium and rhenium metal centres was demonstrated as a proof of concept to achieve novel original supramolecular assemblies. Indeed, substitution of the *trans* chlorine atom of the metal allenylidene precursor with an acetylide or another allenylidene carbon-rich chain, as well as

connection to metal units bearing other carbon-rich ligands should allow the building of large homo/heteronuclear multi-component assemblies. The optical properties of the building blocks are retained in the new adducts, and importantly these complexes show reversible electrochemical behaviour especially for the reduction of the allenylidene chain. Therefore, these results also open the door to the realization of novel magnetic assemblies: (i) with the connection of several allenylidene building blocks around coordination centres, and (ii) with the use of paramagnetic metallic components.

4. Experimental

The reactions were carried out under inert atmosphere using Schlenk techniques. Solvents were freshly distilled under argon using standard procedures. Chromatography and filtration were performed using alumina (Acros, actived neutral 50–200 μm). Electrochemical studies were carried out under argon using an Eco Chemie Autolab PGSTAT 30 potentiostat (CH_2Cl_2, 0.1 M Bu_4NPF_6). The working electrode was a Pt disk, and ferrocene was the internal reference. High resolution mass spectra (HRMS) were recorded in Rennes at the CRMPO (Centre Régional de Mesures Physiques de l'Ouest) on a ZabSpecTOF (LSIMS at 4 kV) spectrometer. The $(bpy)_2RuCl_2$ [57], (^{t}Bu-bpy)$_2RuCl_2$ [58], [RuCl(dppe)$_2$][TfO] (**3**) [59] precursors were prepared as previously reported, and 4,5-diazafluoren-9-one (98%) was purchased from Aldrich.

4.1. H–C≡C–OHC$_{11}$H$_6$N$_2$ (**2**)

In a Schlenk tube, THF (20 mL) was cooled at −78 °C before addition of ethyne measured with a gas burette (40 mmol) and ^{n}BuLi (12.4 mmol, 8 mL of 1.6 M solution in hexane). The mixture was stirred for 15 min at −78 °C before addition of a suspension of 4,5-diazafluoren-9-one (4.17 mmol, 760 mg) in THF (10 mL). The resulting mixture was further stirred for 1 h at −78 °C and 18 h at room temperature before being hydrolyzed with a saturated NH_4Cl solution. The crude product was extracted with CH_2Cl_2 (4 × 50 mL), washed with water (3 × 20 mL), dried, and the solvent was evaporated. Further purification was achieved by chromatography over silica gel (10% diethyl-ether in *n*-pentane) to afford 740 mg of **2** (85%).^{1}H NMR ($CDCl_3$): δ 8.69 (dd, $^2J_{HH}$ = 4.9 Hz, $^3J_{HH}$ = 1.2 Hz, 2H, diazafluorene), 8.08 (dd, $^2J_{HH}$ = 7.7, $^3J_{HH}$ = 1.2 Hz, 2H, diazafluorene), 7.33 (dd, $^2J_{HH}$ = 4.9 and 7.7 Hz, 2H, diazafluorene), 3.20 (br, 1H, OH), 2.52 (s, 1H, CH). ^{13}C{^{1}H} NMR ($CDCl_3$): δ 156.68, 155.80, 141.70, 132.07, 124.21 (Ar), 82.02 (C≡C–H), 72.20 (C≡C–H), 70.91 (C–OH). IR (cm^{-1}, KBr): 2102 ($\nu_{C\equiv C}$). MS(EI) (*m*/*z*): 208.0623 ([M$^+$], calc.: 208.0636).

4.2. [Cl–Ru(dppe)$_2$=C=C=C$_{11}$H$_6$N$_2$][OTf] (**4**)

In a Schlenk tube, [Ru(dppe)$_2$Cl][OTf] (**3**) (1 mmol, 1.08 g) and **2** (1.4 mmol, 291 mg) were dissolved in CH_2Cl_2 (50 mL) and the solution was stirred at room temperature for 72 h. After evaporation, the solid was washed with Et_2O (2 × 20 mL) and crystallization from CH_2Cl_2/Et_2O/*n*-pentane (20:10:40) yielded to 1.08 g of **4** as dark red crystals (83%). ^{31}P{^{1}H} NMR ($CDCl_3$): δ 37.2 (s). ^{1}H NMR (CD_2Cl_2): δ 8.84 (d, $^2J_{HH}$ = 4.1 Hz, 2H, H-diazafluorene), 7.33–6.75 (m, 42H, diazafluorene and Ar), 6.56 (d, $^2J_{HH}$ = 7.1 Hz, 2H, diazafluorene), 3.30 and 3.20 (m, 8H, dppe). ^{13}C{^{1}H} NMR (CD_2Cl_2): δ 320.8 (quint., $^2J_{PC}$ = 15 Hz, Ru=*C*), 249.0 (Ru=C=*C*), 147.2 (Ru=C=C=*C*), 163.6–124.8 (C_{Ar}), 121.05 (q, CF_3SO_3, $^1J_{CF}$ = 320 Hz), 28.3 (quint., dppe, $|^1J_{PC} + {}^3J_{PC}|$ = 22 Hz). IR (cm^{-1}, KBr): 1915 ($\nu_{C=C=C}$). HR-MS(LSIMS) (*m*/*z*): 1123.2007 ([M$^+$], calc.: 1123.1970). Anal. Calc. for $C_{66}H_{54}F_3ClO_3P_4SN_2Ru \cdot 0.5CH_2Cl_2$: C, 60.73; H, 4.22. Found: C, 60.69; H, 4.29%.

4.3. [Cl–Ru(dppe)$_2$=C=C=C$_{11}$H$_6$N$_2${(bpy)$_2$Ru}][B(C$_6$F$_5$)$_4$]$_3$ (**5a**)

In a Schlenk tube, (2,2′-bpy)$_2RuCl_2$ (0.067 mmol, 35 mg) and **4** (0.067 mmol, 85 mg) were heated at reflux in EtOH (5 mL) for 6 h. After cooling down to room temperature, $KB(C_6F_5)_4$ (0.268 mmol, 192 mg) was added and the mixture was kept stirring for 45 min. After evaporation, the residue was dissolved in CH_2Cl_2 (10 mL), the solution was filtered and washed with water (3 × 10 mL). After evaporation of the solvents and washing of the residue with Et_2O (3 × 10 mL), crystallization from CH_2Cl_2/*n*-pentane (15:30) led to 117 mg of **5a** as a brown powder (79%). ^{31}P{^{1}H} NMR ($CDCl_3$): δ 35.7 (s). ^{1}H NMR ($CDCl_3$): δ 8.45–6.77 (m, 60H, Ar), 6.54 (d, $^2J_{HH}$ = 7.7 Hz, 2H, diazafluorene), 3.31 and 2.97 (m, 8H, dppe). IR (cm^{-1}, KBr): 1899 ($\nu_{C=C=C}$). HR-MS(LSIMS) (*m*/*z*): 2895.1980 ([C^{3+}, 2A$^-$]$^+$, calc.: 2895.2000). Anal. Calc. for $C_{157}H_{70}F_{60}ClP_4B_3N_6Ru_2 \cdot 3CH_2Cl_2$: C, 50.19; H, 2.00. Found: C, 50.57; H, 2.02%.

4.4. [Cl–Ru(dppe)$_2$=C=C=C$_{11}$H$_6$N$_2${(^{t}Bu-bpy)$_2$Ru}][PF$_6$]$_3$ (**5b**)

In a Schlenk tube, (4,4′-^{t}Bu$_2$-2,2′-bpy)$_2RuCl_2$ (0.275 mmol, 200 mg) and **4**(0.275 mmol, 350 mg) were heated at reflux in EtOH (20 mL) for 6 h. After cooling down to room temperature, NH_4PF_6 (1.375 mmol, 220 mg) was added and the solution was further stirred for 45 min. The solvent was removed and the residue dissolved in a minimum of CH_2Cl_2. After filtration, the solvent was evaporated and the solid washed with Et_2O (3 × 15 mL). Crystallization from CH_2Cl_2/*n*-pentane (25:50) led to 465 mg of **5b** as a brown powder (77%).^{31}P{^{1}H} NMR ($CDCl_3$): δ 36.1 (s). ^{1}H NMR (CD_2Cl_2): δ 8.32–6.89 (m, 58H, Ar), 6.52 (d, $^2J_{HH}$ = 7.7 Hz, 2H, diazafluorene), 3.22 and 3.03 (m, 8H, dppe), 1.53 and 1.49 (s, 18H, CH_3).^{13}C{^{1}H} NMR (CD_2Cl_2): δ 324.2 (quint., $^2J_{PC}$ = 15 Hz, Ru=*C*), 283.6 (Ru=C=*C*), 166.6–120.8 (Ar), 28.7 (quint., dppe, $|^1J_{PC} + {}^3J_{PC}|$ = 22 Hz) 35.6 and 35.5 (*C*Me$_3$), 30.1 and 30.3 (CH_3). IR (cm^{-1}, KBr): 1900 ($\nu_{C=C=C}$). HR-MS(LSIMS) (*m*/*z*): 2051.4194 ([C^{3+}, 2A$^-$]$^+$, calc.: 2051.4214). Anal. Calc. for $C_{157}H_{70}F_{60}ClP_4B_3N_6Ru_2 \cdot 0.5CH_2Cl_2$: C, 54.45; H, 4.64. Found: C, 54.39; H, 4.59%.

4.5. [Cl–Ru(dppe)$_2$=C=C=C$_{11}$H$_6$N$_2${Re(CO)$_3$Cl}][OTF] (**6**)

In a Schlenk tube, $Re(CO)_5Cl$ (0.15 mmol, 58 mg) and **4** (0.15 mmol, 194 mg) were heated at reflux in toluene (20 mL) for 18 h. The mixture was concentrated, washed with *n*-pentane (20 mL) and filtered. After evaporation, the solid was washed with Et_2O (2 × 20 mL). Crystallization from CH_2Cl_2/*n*-pentane (1:2) yielded 160 mg of **6** as dark brown crystals (67%). ^{31}P{^{1}H} NMR ($CDCl_3$): δ 35.5 (s). ^{1}H NMR (CD_2Cl_2): δ 8.90 (d, $^2J_{HH}$ = 4.8 Hz, 2H, diazafluorene), 7.41–6.90 (m, 42H, diazafluorene and Ar), 6.77 (d, $^2J_{HH}$ = 7.2 Hz, 2H, diazafluorene), 3.35 and 3.20 (m, 8H, dppe). ^{13}C{^{1}H} NMR (CD_2Cl_2): δ 324.6 (quint., $^2J_{PC}$ = 14 Hz, Ru=*C*), 281.2 (Ru=C=*C*), 198.4 and 189.1 (CO), 166.16–128.2 (Aromatics), 121.15 (q, CF_3SO_3, $^1J_{CF}$ = 320 Hz), 28.7 (quint., dppe, $|^1J_{PC} + {}^3J_{PC}|$ = 22 Hz). IR (cm^{-1}, KBr): 2024 (s) (ν_{CO}), 1918 (vs) (ν_{CO}), 1897 ($\nu_{C=C=C}$), 1885 (s) (ν_{CO}). HR-MS(LSIMS) (*m*/*z*): 1429.1058 ([C]$^+$, calc.: 1429.1063). Anal. Calc. for $C_{69}H_{54}F_3Cl_2O_6P_4SN_2ReRu \cdot 0.5CH_2Cl_2$: C, 52.51; H, 3.42. Found: C, 51.15; H, 3.45%.

Acknowledgement

We thank the CNRS and the Université de Rennes 1 for financial support.

Appendix. Supplementary material

CCDC 663046 contains the supplementary crystallographic data for this paper. These data can be obtained free of charge from The

Cambridge Crystallographic Data Centre via www.ccdc.cam.ac.uk/data_request/cif. Supplementary data associated with this article can be found, in the online version, at doi:10.1016/j.jorganchem.2008.03.014.

References

[1] C. Creutz, B.S. Brunschwig, N. Sutin, Comprehensive Coordination Chemistry II: From Biology to Nanotechnology, vol. 7, Elsevier/Pergamon, Oxford, New York, 2004.
[2] J.-P. Launay, Chem. Soc. Rev. 30 (2001) 386–397.
[3] K.D. Demadis, C.M. Hartshorn, T.J. Meyer, Chem. Rev. 101 (2001) 2655–2685.
[4] J.-M. Lehn, Supramolecular Chemistry – Concepts and Perspectives, VCH, Weinheim, 1995.
[5] W. Kaim, G.K. Lahiri, Angew. Chem., Int. Ed. 46 (2007) 1778–1796.
[6] F.A. Cotton, C.Y. Liu, C.A. Murillo, D. Villagrán, X. Wang, J. Am. Chem. Soc. 126 (2004) 14822–14831.
[7] D.M. D'Alessandro, F.R. Keene, Chem. Rev. 106 (2006) 2270–2298.
[8] J.-P. Sauvage, J.-P. Collin, J.-C. Chambron, S. Guillerez, C. Coudret, V. Balzani, F. Barigelletti, L. De Cola, L. Flamigni, Chem. Rev. 94 (1994) 993–1019.
[9] R. Ziessel, M. Hissler, A. El-Ghaoury, A. Harriman, Chem. Soc. Rev. 178–180 (1998) 1251–1298.
[10] V. Balzani, A. Juris, M. Venturi, S. Campagna, S. Serroni, Chem. Rev. 96 (1996) 759–833.
[11] F. Paul, C. Lapinte, Coord. Chem. Rev. 178–180 (1998) 431–509.
[12] S. Szafert, J.A. Gladysz, Chem. Rev. 106 (2006) PR1–PR33.
[13] K. Venkatesan, O. Blacque, H. Berque, Dalton Trans. (2007) 1091–1100.
[14] T. Ren, Organometallics 24 (2005) 4854–4870.
[15] N.J. Long, C.K. Williams, Angew. Chem., Int. Ed. 42 (2003) 2586–2617.
[16] M.I. Bruce, P.J. Low, Adv. Organomet. Chem. 50 (2004) 179–444.
[17] S. Rigaut, D. Touchard, P.H. Dixneuf, in: T. Hirao (Ed.), Redox Systems Under Nano-Space Control, Springer, Heidelberg, 2006, pp. 55–79.
[18] S. Rigaut, D. Touchard, P.H. Dixneuf, Coord. Chem. Rev. 248 (2004) 1585–1601.
[19] H. Werner, Chem. Commun. (1997) 903–910.
[20] M.I. Bruce, Chem. Rev. 98 (1998) 2797–2858.
[21] V. Cadierno, M.P. Gamasa, J. Gimeno, Eur. J. Inorg. Chem. (2001) 571–591.
[22] J.P. Selegue, Coord. Chem. Rev. 248 (2004) 1543–1563.
[23] N. Mantovani, M. Brugnati, L. Gonsalvi, E. Grigiotti, F. Laschi, L. Marvelli, M. Peruzzini, G. Reginato, R. Rossi, P. Zanello, Organometallics 24 (2005) 405–418.
[24] C.-Y. Wong, G.S.M. Ming, C.-M. Che, N. Zhu, Angew. Chem., Int. Ed. 45 (2006) 2694–2698.
[25] S. Rigaut, D. Touchard, P.H. Dixneuf, Organometallics 22 (2003) 3980–3984.
[26] S. Rigaut, O. Maury, D. Touchard, P.H. Dixneuf, Chem. Commun. (2001) 373–374.
[27] S. Rigaut, K. Costuas, D. Touchard, J.-Y. Saillard, S. Golhen, P.H. Dixneuf, J. Am. Chem. Soc. 126 (2004) 4072–4073.
[28] S. Rigaut, J. Perruchon, S. Guesmi, C. Fave, D. Touchard, P.H. Dixneuf, Eur. J. Inorg. Chem. (2005) 447–460.
[29] S. Rigaut, C. Olivier, K. Costuas, S. Choua, O. Fadhel, J. Massue, P. Turek, J.-Y. Saillard, P.H. Dixneuf, D. Touchard, J. Am. Chem. Soc. 128 (2006) 5859–5876.
[30] C. Olivier, S. Choua, P. Turek, D. Touchard, S. Rigaut, Chem. Commun. (2007) 3100–3102.
[31] D. Touchard, P. Haquette, A. Daridor, A. Romero, P.H. Dixneuf, Organometallics 17 (1998) 3844–3852.
[32] B.-S. Kim, J.M. Beebe, C. Olivier, S. Rigaut, D. Touchard, J.G. Kushmerick, X.Y. Zhu, C.D. Frisbie, J. Phys. Chem. C 111 (2007) 7521–7526.
[33] F. Paul, C. Lapinte, in: M. Gielen, R. Willem, B. Wrackmeyer (Eds.), Unusual Structures and Physical Properties in Organometallic Chemistry, John Wiley & Sons, London, 2002, p. 220.
[34] F. Paul, S. Goeb, F. Justeaud, G. Argouarch, L. Toupet, R. Ziessel, C. Lapinte, Inorg. Chem. 46 (2007) 9036–9038.
[35] Z.-N. Chen, Y. Fan, J. Ni, Dalton Trans. (2008) 573–581.
[36] K. Welter, J. Brunner, W. Hofstraat, L. De Cola, Nature 21 (2003) 54–57.
[37] R. Argazzia, N.Y. Murakami Ihac, H. Zabrid, F. Odobeld, C.A. Bignozzi, Coord. Chem. Rev. 248 (2004) 1299–1316.
[38] T. Le Bouder, O. Maury, A. Bondon, K. Costuas, E. Amouyal, I. Ledoux, J. Zyss, H. Le Bozec, J. Am. Chem. Soc. 125 (2003) 12284–12299.
[39] D.J. Stufkens, A. Vlcek Jr., Coord. Chem. Rev. 177 (1998) 127–179.
[40] I.E. Pomestchenko, D.E. Polyansky, F.N. Castellano, Inorg Chem. 44 (2005) 3412–3421.
[41] S.H.-F. Chong, S.C.-F. Lam, V.W.-W. Yam, N. Zhu, K.-K. Cheung, S. Fathallah, K. Costuas, J.-F. Hallet, Organometallics 23 (2004) 4924–4933.
[42] K.M.C. Wong, S.C.F. Lam, C.-C. Ko, N. Zhu, V.W.W. Yam, S. Roué, C. Lapinte, S. Fathallah, K. Costuas, S. Kahlal, J.-F. Halet, Inorg. Chem. 42 (2003) 7086–7097.
[43] W.-Y. Wong, Coord. Chem. Rev. 249 (2005) 971–997.
[44] Y. Wang, W. Perez, G.Y. Zheng, D.P. Rillema, Inorg. Chem. 37 (1998) 2051–2059.
[45] Y. Wang, W.J. Perez, J. Zhang, D.P. Rillema, C.L. Huber, Inorg. Chem. 37 (1998) 2227–2234.
[46] V.W.-W. Yam, Y. Yang, J. Zhang, B.W.-K. Chu, N. Zhu, Organometallics 20 (2001) 4911–4918.
[47] M.J. Plater, S. Kemp, E. Lattman, J. Chem. Soc., Perkin Trans 1 (2000) 971–979.
[48] As very often observed for complexes of this kind, inclusion solvent is observed despite thorough pumping, preventing good elemental analysis.
[49] The contribution of the disordered solvents to the calculated structure factors was estimated following the BYPASS algorithm, implemented as the SQUEEZE option in PLATON. A new data set, free of solvent contribution, was then used in the final refinement. See: P.v.d. Sluis, A.L. Spek, Acta Cryst. A 46 (1990) 194–201;
A.L. Spek, Acta Crystallogr., Sect A 46 (1990) C34.
[50] J.P. Selegue, Organometallics 1 (1982) 217–218.
[51] M. Riklin, A. von Zelewsky, Helv. Chim. Acta. 79 (1996) 2176–2179.
[52] R.F. Winter, K.W. Klinkhammer, S. Zalis, Organometallics 20 (2001) 1317–1333.
[53] R. Ziessel, A. Juris, M. Venturi, Inorg. Chem. 37 (1998) 5061–5069.
[54] J.F. Berry, F.A. Cotton, C.A. Murillo, Organometallics 23 (2004) 2503–2506.
[55] N. Auger, D. Touchard, S. Rigaut, J.-F. Halet, J.-Y. Saillard, Organometallics 22 (2003) 1638–1644.
[56] J.C. Luong, L. Nadjo, M.S. Wrighton, J. Am. Chem. Soc. 100 (1978) 5790–5795.
[57] V. Aranyos, A. Hagfeldt, H. Grennberg, E. Figgemeier, Polyhedron 23 (2004) 589–598.
[58] T. Ben Hadda, H. Le Bozec, Polyhedron 7 (1988) 575–577.
[59] J.R. Polam, L.C. Porter, J. Coord. Chem. 29 (1993) 109–119.